ADVANCES IN ATMOSPHERIC SCIENCES, VOL. 39, APRIL 2022, 553–565

• News & Views •

Extreme Cold Events from East Asia to North America in Winter 2020/21: Comparisons, Causes, and Future Implications※

Xiangdong ZHANG*[1], Yunfei FU[2], Zhe HAN[3], James E. OVERLAND[4], Annette RINKE[5], Han TANG[1], Timo VIHMA[6], and Muyin WANG[4,7]

[1]*Univeristy of Alaska Fairbanks*, *Fairbanks*, *AK* 99775, *USA*

[2]*University of Science and Technology of China*, *Hefei* 230026, *China*

[3]*Institute of Atmospheric Physics*, *Chinese Academy of Sciences*, *Beijing* 100029, *China*

[4]*NOAA/Pacific Marine Environmental Laboratory*, *Seattle*, *WA* 98115, *USA*

[5]*Alfred Wegener Institute*, *Helmholtz Center for Polar and Marine Research*, 14401 *Potsdam*, *Germany*

[6]*Finnish Meteorological Institute*, *FI*-00101 *Helsinki*, *Finland*

[7]*University of Washington*, *Seattle*, *WA* 98105, *USA*

(Received 15 June 2021; revised 27 June 2021; accepted 5 July 2021)

ABSTRACT

Three striking and impactful extreme cold weather events successively occurred across East Asia and North America during the mid-winter of 2020/21. These events open a new window to detect possible underlying physical processes. The analysis here indicates that the occurrences of the three events resulted from integrated effects of a concurrence of anomalous thermal conditions in three oceans and interactive Arctic-lower latitude atmospheric circulation processes, which were linked and influenced by one major sudden stratospheric warming (SSW). The North Atlantic warm blob initiated an increased poleward transient eddy heat flux, reducing the Barents-Kara seas sea ice over a warmed ocean and disrupting the stratospheric polar vortex (SPV) to induce the major SSW. The Rossby wave trains excited by the North Atlantic warm blob and the tropical Pacific La Nina interacted with the Arctic tropospheric circulation anomalies or the tropospheric polar vortex to provide dynamic settings, steering cold polar air outbreaks. The long memory of the retreated sea ice with the underlying warm ocean and the amplified tropospheric blocking highs from the midlatitudes to the Arctic intermittently fueled the increased transient eddy heat flux to sustain the SSW over a long time period. The displaced or split SPV centers associated with the SSW played crucial roles in substantially intensifying the tropospheric circulation anomalies and moving the jet stream to the far south to cause cold air outbreaks to a rarely observed extreme state. The results have significant implications for increasing prediction skill and improving policy decision making to enhance resilience in "One Health, One Future".

Key words: extreme weather events, sea surface temperature, Arctic sea ice, Arctic amplification, sudden stratospheric warming, stratospheric polar vortex

Citation: X. D. Zhang, Y. F. Fu, Z. Han, J. E. Overland, A. Rinke, H. Tang, T. Vihma, and M. Y. Wang, 2022: Extreme cold events from East Asia to North America in winter 2020/21: Comparisons, causes, and future implications. *Adv. Atmos. Sci.*, **39**(4), 553–565, https://doi.org/10.1007/s00376-021-1229-1.

1. Introduction

Striking extreme cold weather events successively occurred across the Northern Hemisphere continents during the mid-winter of 2020/21. Specifically, two pronounced cold air outbreaks consecutively swept from Siberia to East Asia during the period of late December of 2020 to mid-January of 2021, causing record-breaking cold surface air temperatures (SATs) with strong winds over broad areas. Extremely cold temperatures of –19.6°C and –19.9°C were observed on 7 January 2021 in Beijing and Tianjin, China, respectively, setting new records in these two locations for 7 January after their previously set-

※ This paper is a contribution to the special issue on Extreme Cold Events from East Asia to North America in Winter 2020/21.

* Corresponding author: Xiangdong ZHANG
Email: xzhang9@alaska.edu

ting records on the same date in 1967 [China Meteorological Administration, http://www.cma.gov.cn/2011wmhd/2011wzbft/2011wftzb/202101/t20210107_569795.html (in Chinese)]. Even worse, historical snow/ice storms and associated cold airmasses struck the Great Plains and the Deep South of North America in the following February of 2021. As a result, the lowest temperatures ever and their persistence over an unexpectedly long time period were recorded in the Southern United States, such as Texas and Oklahoma. For example, the temperature reached –13.3°C and –8.3°C in Austin and Houston on 15 February, breaking their previous coldest records on that date of 15 February of –6.7°C and –7.8°C from 1908 and 1905, respectively (Valentine's Week Winter Outbreak 2021: Snow, Ice, & Record Cold, the U.S. National Weather Service, https://www.weather.gov/hgx/2021ValentineStorm). The disastrous snow/ice storms and the resulting power outages significantly impacted daily life, caused tremendous damage to economy and infrastructure, and resulted in151 deaths in Texas (Texas Department of State Health Services).

The severity and significantly high socioeconomic impacts of these three cold events are rarely, if not unprecedentedly, observed on the same dates or even for the entire winter season during the last half to full century. However, extreme cold winter weather events of different intensities have become more frequent in both Eurasia and North America during recent decades (e.g., the recent reviews by Cohen et al., 2020; Vihma et al., 2020; Zhang et al., 2020; Overland et al., 2021). The ostensible increase in the frequency of occurrence of extreme cold winter events has greatly motivated and led to a rapidly growing body of research on the topic, particularly on considering the puzzling questions regarding the occurrence of extremely cold temperatures associated with these events against the long-term global warming trend. The leading, fundamental problem therefore becomes whether the increase in the frequency of extreme cold events results from an externally forced warming climate or natural variability in the climate system.

To address the problem, a number of scientific hypotheses have been proposed, and a great amount of research results have been delivered. The majority of these studies have focused on testing the hypothesis that Arctic amplification of global warming (consisting of surface/lower-tropospheric air temperature increases and accompanying sea ice decline) has forced the increased occurrence of winter extreme cold events through a polarity or spatial transformation of the atmospheric circulation (e.g., Thompson and Wallace, 1998; Zhang et al., 2008; Wu and Zhang, 2010; Overland et al., 2015), alteration of jet streams and planetary waves (e.g., Barnes and Screen, 2015; Francis and Vavrus, 2015; Vavrus et al., 2017; Woollings et al., 2018), changes in synoptic scale cyclones, anticyclones, and Ural Mountains/Greenland blocking highs (e.g., Zhang et al., 2012; Hanna et al., 2016; Luo et al., 2016; Tyrlis et al., 2019), or strengthened stratosphere–troposphere interactions (e.g., Kim et al., 2014; Kretschmer et al., 2018; Zhang et al., 2018a). Meanwhile, "tug-of-war" effects between Arctic and low-latitude forcings have also been proposed and investigated (Barnes and Polvani, 2015). It is found that tropical Pacific SST anomalies and the stratospheric quasi-biennial oscillation (QBO) also modulate changes in the midlatitude atmospheric circulation, jet stream waves, and storm tracks (e.g., Basu et al., 2013; Yamazaki et al., 2020).

Despite rapidly accumulating research results, there are still discrepancies, inconsistencies, and even strong debates (e.g., McCusker et al., 2016; Screen et al., 2018; Blackport et al., 2020; Cohen et al., 2020). The highly limited sample size of extreme cold events in the warming climate is one of the major impediments to establishing observational cause–effect evidence and constraining modeling uncertainties. Due to their extremeness, breaking of many records, and successive occurrence across the Eurasian and North American continents, the 2020/21 events provide a new, unique opportunity to augment observational evidence, detect the possible underlying physical processes, and further fuel research on the topic to move toward a consensus.

2. Datasets and methodology

The data used here include hourly SAT and geopotential height (GHT) at 300 hPa and 50 hPa from the fifth generation European Center for Medium Range Forecasting Reanalysis (ERA5; Hersbach et al., 2020), which have a spatial resolution of 0.25° and are available from 1 January 1979 to present. Based on these data, we constructed their winter (1 December–28 February) daily means. The 30-year time period of 1979/80–2008/09 was chosen as the reference to form the winter daily mean climatology of these parameters. Monthly sea ice concentrations at a resolution of 25 km were obtained from the Sea Ice Concentration from Nimbus-7 SMMR and DMSP SSM/I-SSMIS Passive Microwave Data, version 1 (Cavalieri et al., 1996) and the Near-Real-Time DMSP SSMIS Daily Polar Gridded Sea Ice Concentrations datasets (Maslanik and Stroeve, 1999). The former covers a period of October 1978–December 2020. The latter provides the near-real-time data for January and February 2021. Monthly mean sea surface temperatures (SSTs) from the Extended Reconstructed Sea Surface Temperature (ERSST), version 5, at a resolution of 2.0° (Huang et al., 2017a) were also used in this analysis. The minimum SAT can occur at different locations in different winters. To minimize uncertainties in defining extreme events, we used the regional average of the daily mean SAT to evaluate the level of the extremeness of the temperature anomaly events, including the three events in winter 2020/21 discussed in this study.

3. Extremeness of the 2020/21 cold winter events

A number of cold spells occurred in the winter of 2020/21. Two of these events occurred over East Asia (25–31 December 2020 and 5–10 January 2021), and one occurred over North America (5–22 February 2021). As mentioned in section 1, these events exhibited extraordinary extremeness in terms of intensity, duration, and socioeconomic impacts. During these three events, low temperatures exceeded two standard deviations over large areas in both regions, reaching the lowest area-averaged values on 30 December 2020 and 7 January 2021 in East Asia and for the period of 12–15 February 2021 in North America (Fig. 1). The most prominent characteristics of these cold air outbreaks are their far-reaching southward extensions of cold airmasses, though the coldest SAT still stayed in the north of the study areas. Compared with the climatology from 1979/80–2008/09, the freezing temperature contour lines moved from about 35°–40°N to 30°N in eastern China and from about 38°N to 30°N over the Great Plains of the United States.

The southward extents of the cold airmasses can also be described by the spatial distribution of the SAT anomalies (Figs. 1d–f). In East Asia, a large negative SAT anomaly center can be observed in the south around 30°–35°N around the east coast of China on 30 December 2020 and 7 January 2021, where the SAT decreased by more than 13°C. Large negative SAT anomalies can also be found to the south of 30°N in North America on 12–15 February 2021, with an even larger decrease in temperature (about 20°C) compared to the events in East Asia.

To evaluate the intensity of these three events compared with all historical temperature anomalies, we conducted a probability density function (PDF) analysis of the regionally averaged daily SAT anomalies for the last 42 years (Fig. 2). The regionally averaged SAT anomalies approximately range from –6.0°C to 6.0°C in East Asia and from –8.0°C to 7.5°C in North America. The anomalies were about –4.0°C and –4.5°C over the East Asian area on 30 December 2020 and 7 January 2021, respectively. An even colder anomaly of –6.4°C occurred over the North American area. All of these values are close to the coldest tail in their respective PDF distributions. The skewed Gaussian-fitting PDF shows these three cold events at 2nd, 3rd, and 1st percentiles among all 42 years of winter daily temperature anomaly events. This suggests that they are certainly small probability events, indicating their level of extremeness during the past 42 winters.

During the most recent decade, there has been a warming shift of SATs with an obvious increase in the frequency of positive SAT anomalies in both East Asia and North America (Fig. 2). However, this change demonstrates a difference for the cold SAT anomalies between the two regions. There is almost no change in the frequency of cold SAT anomalies, espe-

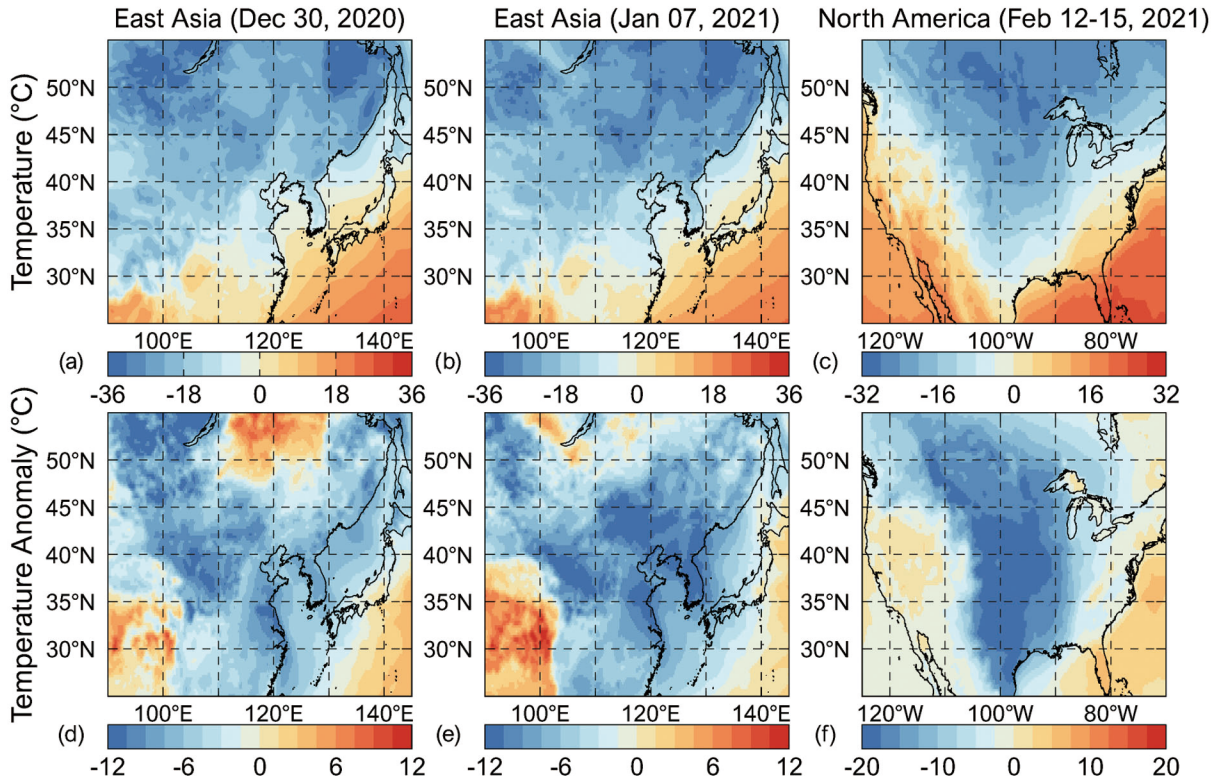

Fig. 1. Daily mean surface air temperature (SAT; at 2 m, in °C) on (a) 30 December 2020 and (b) 7 January 2021 in East Asia (90°–145°E; 25°–55°N). (c) Average of daily mean SAT during 12–15 February 2021 in North America (125°–70°W; 25°–55°N). (d)–(f) the same as (a)–(c) but for the SAT anomalies. The daily anomalies were calculated relative to the daily mean climatology constructed for the time period of 1979/80–2008/09.

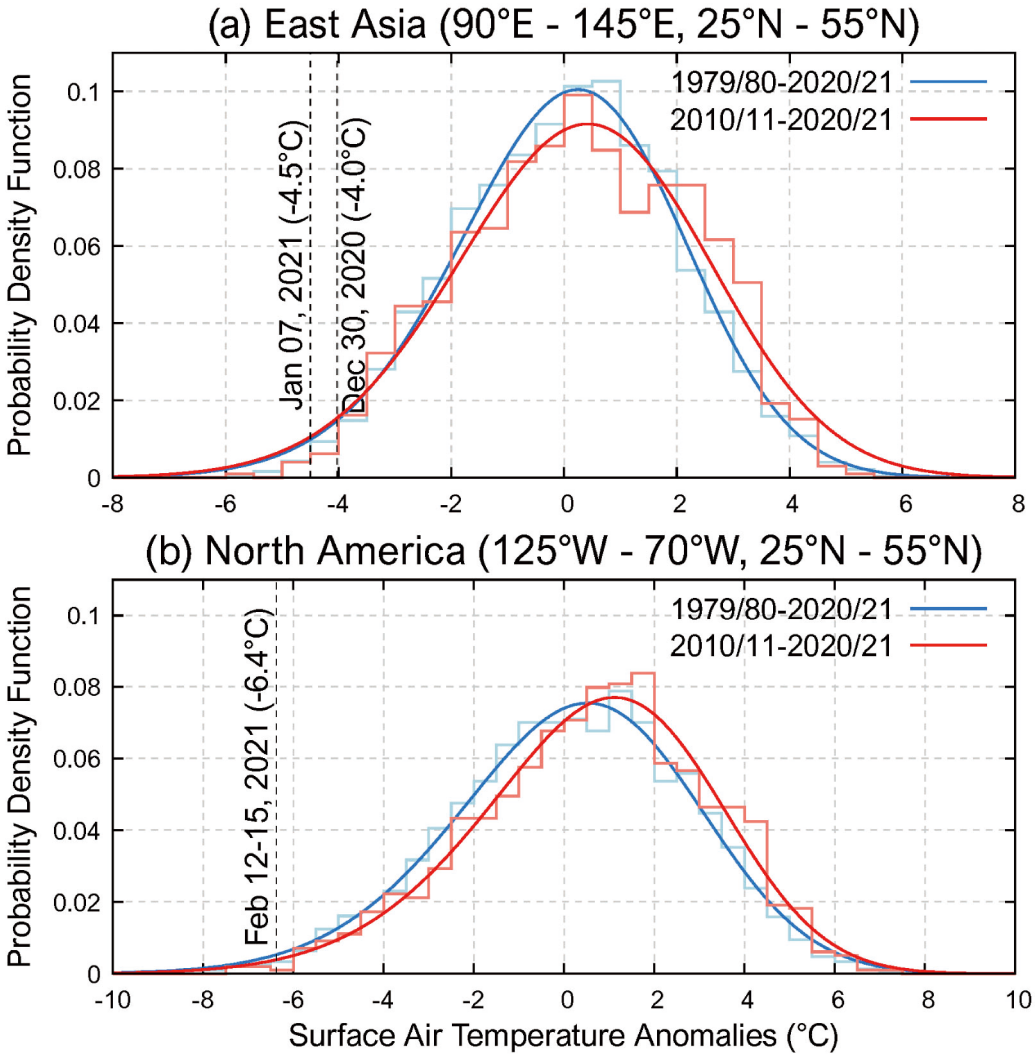

Fig. 2. The probability density function (PDF; histograms and the skewed Gaussian fitting) of winter (1 December–28 February) daily mean SAT anomalies (relative to the daily mean climatology from 1979/80–2008/09) averaged over (a) East Asia; and (b) North America from 1979/80–2020/21 (blue line) and 2010/11–2020/21 (red line). The East Asia area-averaged daily mean SAT anomalies on 30 December 2020 and 7 January 2021 and the North America area-averaged four-day mean SAT anomalies from 12–15 February 2021 are shown by the vertical dashed lines in (a) and (b), respectively.

cially when they are colder than –2.0°C, in East Asia, while a decrease occurred in North America. This suggests that the long-term global warming trend has not influenced the frequency of occurrence of strong cold events in East Asia, but it has reduced the probability of occurrence of extreme cold events in North America.

4. Driving mechanisms—Integrated effects of multiple processes

It has been a perplexing problem to answer what causes the occurrence of the extreme cold events in the context of the accelerating warming climate (Huang et al., 2017b). The majority of prevailing research on the topic focuses on the emergence of anomalous thermodynamic forcing associated with Arctic warming amplification and sea ice decrease. The central piece of the debate about the problem results from the inconsistence and statistical insignificance in research results about atmospheric circulation responses to these anomalous forcing. In addition, Arctic forcing may interact with tropical/extratropical ocean forcing to further complicate the problem. Therefore, in this study, we first examine the ocean environment conditions and then the atmospheric circulation, as well as possible associations between them.

4.1. *Arctic sea ice and tropical/extratropical ocean forcing*

As an outstanding indicator of Arctic warming amplification, sea ice decrease adds additional surface thermodynamic for-

cing to the overlying atmospheric circulation. When looking at sea ice data since 1979, we found that the sea ice extent in the winter of 2020/21 was considerably smaller than its climatology (Fig. 3a). Specifically, the sea ice area in the Barents–Kara seas reached its lowest value on record, particularly in the month of December 2020. On the North Pacific Arctic side (i.e., the Bering–Chukchi–Beaufort seas), the sea ice area also shows the second lowest value over the past 42 years. Considering the nature of the poleward intrusion of the North Atlantic and North Pacific warm water into these two ocean areas and absorbed heat energy through open water during the prior summer season, the greater retreat of sea ice cover in these areas would lead to a larger increase in turbulent heat fluxes and upwelling longwave radiation to the atmosphere.

At the same time, large SST anomalies occurred from the tropical Pacific Ocean to the North Atlantic Arctic in winter 2020/21 (Fig. 3b). One of the most prominent phenomena was a strong La Niña with a cold tongue of SST anomalies ranging from the eastern to the central tropical Pacific Ocean. This La Niña was developed from September 2020 throughout March 2021 (https://www.cpc.ncep.noaa.gov/products/analysis_monitoring/enso_advisory/ensodisc.shtml). Large warm SST anomalies also appeared outside the Niño regions (0°–10°S, 90°W–80°W; 5°N–5°S, 160°E–90°W), extending from the western tropical Pacific to the northeastern North Pacific. A warm blob with a maximum SST anomaly of 3.5°C was present in the Gulf of Alaska and off the west coast of North America.

Other notable ocean thermal anomalies are the warm blob off the east coast of North America and the cold anomaly near the southern tip of Greenland in the North Atlantic Ocean. A warm SST anomaly also occurred from the Norwegian Sea to the Barents–Kara seas, in correspondence to the substantially retreated sea ice there. When examining the temporal evolution of their intensities, we found that all of these North Atlantic and Arctic SST anomalies were at their strongest state in December 2020 and then gradually weakened at a slow pace in the following two months.

4.2. *Tropospheric circulation, Rossby waves, and jet streams*

The tropospheric atmospheric circulation clearly exhibited high GHT anomalies over the Arctic, wave patterns across the North Atlantic and the Eurasian continent, and a southward shift and intensification of the jet stream over East Asia at 300 hPa associated with the occurrence and development of the first East Asia cold event (Figs. 4a1–a6). Initially, an anomalous high center occurred off the east coast of North America with a ridge extending into the Nordic Seas on 25 December 2020, in concert with the warm SST blob in the same location (Fig. 3b). The warm blob could have served as a source of wave activity and excited Rossby wave train propagation, which can be observed on 26 December. As a result, anomalous high and low centers emerged from the northwestern North Atlantic to the Barents–Kara seas. The initially forced ridge and the subsequently developed wave train would enhance poleward transient eddy heat and moisture fluxes into the Arctic, leading to the decrease and minimum of sea ice area in the Barents–Kara seas in December 2020 as mentioned above. During this time period, the East Asian trough became stronger and exhibited a negative GHT anomaly, which can be associated with the increased baroclinicity due to the cold and warm SST anomalies between the Sea of Okhotsk and the rest of the western North Pacific Ocean (Fig. 3b). Meanwhile, the jet stream was located around 40°N over the Japan Sea.

Following the enhanced transient eddy heat influx, the decreased sea ice cover over the warm ocean, and the resultant increase in the surface and lower-tropospheric air temperatures over the Barents–Kara seas (not shown), the high GHT anomalies over the Barents–Kara seas intensified and extended over a large area of the Arctic, as explained by the quasi-geostrophic (QG) theory (Holton, 2004). The anomalous low center over the East Greenland Sea accordingly moved southeastward to the area of the United Kingdom. As a consequence, a zonally aligned wave train developed in the midlatitudes from the North Atlantic to East Asia during the period of 27–30 December. The wave train anchored and amplified the fluctuation of the atmospheric circulation, enhancing blocking highs over eastern Europe and western Siberia (i.e., to the west and

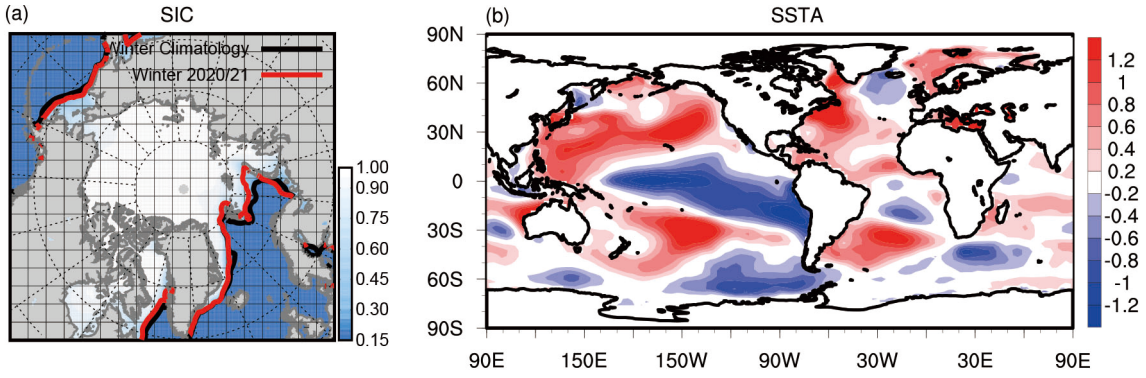

Fig. 3. (a) Climatology (shading) and climatological ice edge (black lines) of winter (December–January–February; 1979/80–2020/21) sea ice concentration and the 2020/21 winter ice edge (red lines). The ice edge is defined by sea ice concentration at 0.15. (b) SST (unit: °C) anomalies in winter 2020/21. The SST anomalies were calculated relative to the climatological mean from 1980/81–2009/10.

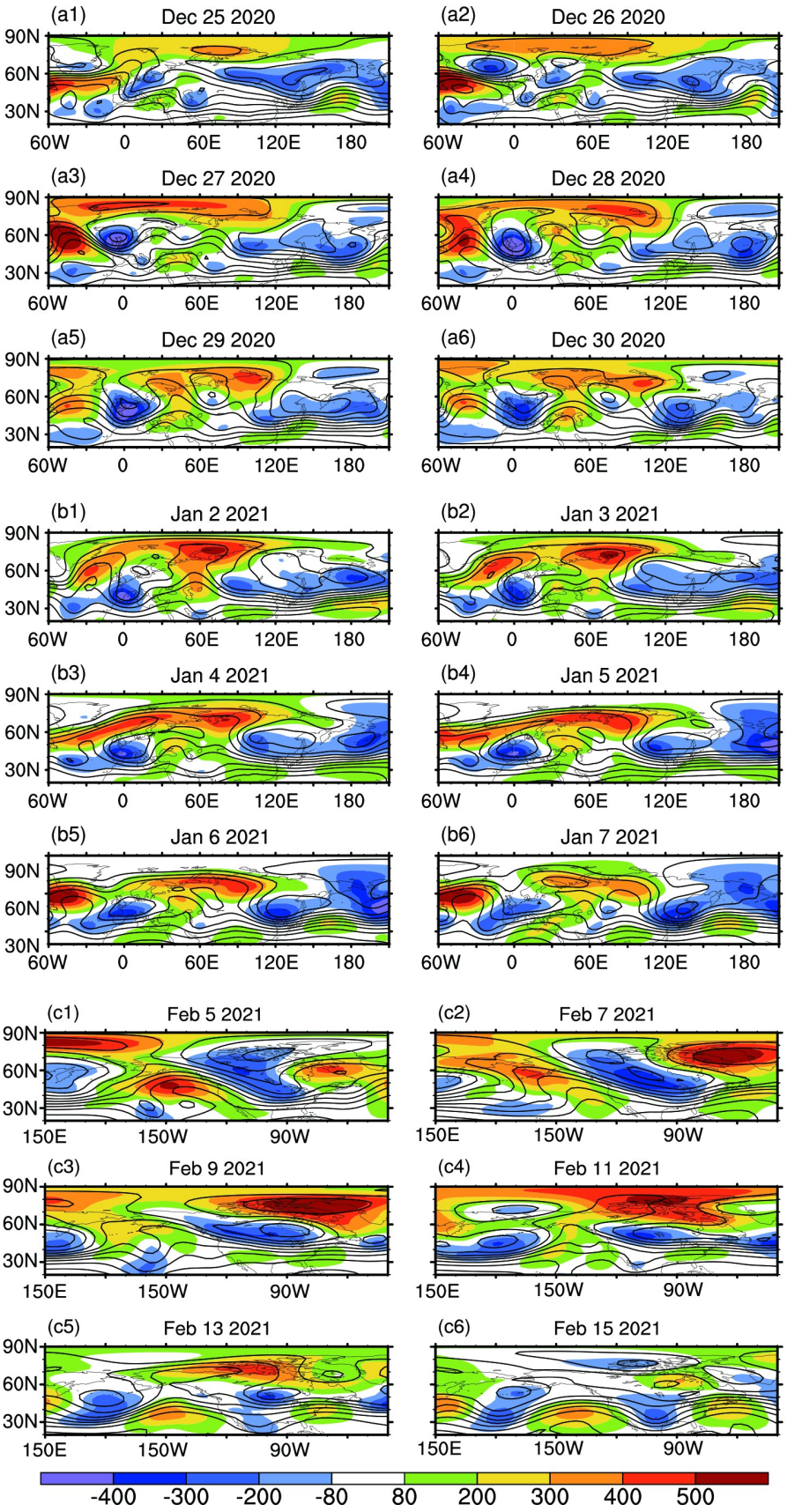

Fig. 4. Geopotential height (solid lines) and its anomalies (relative to the daily mean climatology from 1979/80–2008/09; shading, in meters) at 300 hPa at the selected days prior to the strongest phase of each of the three cold events in East Asia (a1–a6 and b1–b6) and North America (c1–c6) in winter 2020/21.

east sides of the Ural Mountains). Meanwhile, the high Arctic GHT anomaly developed further to the east and then shifted southeastward to the Laptev Sea coastal area. The combination of the western Siberia ridge and the southeastward-shifted Arctic GHT anomaly, together with the rapidly deepened East Asian trough and intensified jet stream over the Japan Sea, strengthened the meridionally oriented circulation over East Asia, triggering a cold air outbreak (Figs. 1 and 2).

The interactions between the Arctic and midlatitude circulations also played an essential role in the occurrence of the second cold event in East Asia. The jet stream was also located relatively to the south, between 30–40°N, from East Asia to the North Pacific. However, their spatial structures, temporal evolutions, and the way in which they interacted demonstrated some obvious differences (Figs. 4b1–b6). Although there were blocking highs over the North Atlantic and Ural Mountains areas since the beginning of the event (2–5 January 2021), the formation and intensification of the meridionally orientated circulation over East Asia was predominately initiated and shaped by the strong positive GHT anomaly over the Kara and Laptev seas and the negative GHT anomaly over East Asia. The southeastward shift of the Arctic anomalous high, the substantial deepening of the East Asian anomalous low (i.e., the East Asian trough), and the intensified jet stream over East Asia from 4–7 January provided an outstanding dynamic setting driving cold polar air to plunge southward. Note that the spatial distribution of the high and low GHT anomalies over the Eurasian high latitudes and the North Pacific Ocean during this event have strong projection on the negative Arctic Rapid change Pattern (ARP), which has played a decisive dynamic role in systematically and simultaneously causing both rapid Arctic warming and cold Eurasia after the late 1990s (Zhang et al., 2008).

During this event, there was also a Rossby wave train originating from the North Atlantic warm blob region propagating southeastward to East Asia; it was especially well-developed from 4–7 January (Figs. 4b3–b6). The anomalous high centers over the North Atlantic and the Ural Mountains linked the midlatitude circulation to the Arctic positive GHT anomalies, resulting in intensified ridges or blocking highs and facilitating increased poleward transient eddy heat flux. The anomalous high center of the wave train reinforced the ridge over western China on 6–7 January, which then strengthened the meridional flow described above, enhancing the cold air outbreak and enabling it to reach southeastern China. In addition, compared with the first cold event, the pathway of the wave train during this event was located over relatively lower latitudes.

The cold event in North America was more severe and lasted longer than the two East Asia events, as analyzed above. The La Niña event preconditioned an anomalous tropospheric circulation from the central tropical Pacific to the North Pacific and North America. In January and early February 2021, the Niño 4 (5°N–5°S, 150°W–160°E) regional mean SST anomalies reached large negative values exceeding –1.0°C (as low as –1.4°C in mid-January) (https://www.cpc.ncep.noaa.gov/products/analysis_monitoring/enso_advisory/ensodisc.shtml). As a result, the Pacific/North American (PNA) index became negative from 21 January to 9 February (https://www.cpc.ncep.noaa.gov/products/precip/CWlink/pna/pna.shtml). Correspondingly, a negative PNA teleconnection pattern (i.e., a Rossby wave train) emanated from the central tropical Pacific Ocean and propagated to the northeastern North Pacific, the central part of North America, and Eastern Canada (van den Dool et al., 2000; Fig. 4c1). At the same time, the atmospheric circulation anomalies originating from the Arctic further transformed the midlatitude circulation anomalies. A strong low-pressure system, or a tropospheric polar vortex (TPV, a recently coined name to be distinguished from the stratospheric polar vortex, SPV), occurred over the Canadian Arctic Archipelago, which meridionally stretched and deepened the low center of the PNA pattern over the North American continent. The atmospheric circulation was therefore predominantly characterized by a ridge over the eastern North Pacific, a trough ranging from the Canadian Arctic Archipelago down to the Great Plains and the Southern United States, and a southward shifted and intensified jet stream over the southern area of the United States, driving cold air southward.

During the following days, the poleward extended ridges over the North Pacific and Eastern Canada/Baffin Bay favored warm air advection into the Arctic, leading to increased thickness of the Arctic air column according to the QG theory (Holton, 2004) and as seen in Figs. 4c2–c4. The negative PNA pattern then gradually weakened and was deformed. Nevertheless, the North Pacific ridge was further intensified, extending into the Gulf of Alaska, the Bering Sea, Alaska, and the Chukchi Sea. The TPV over North America deepened and shifted southward. The blocking high strengthened over Baffin Bay and Greenland. As a consequence, cold air was persistently transported southward over the North American continent. Note that during this period an anomalous low center developed and intensified over the western North Pacific, shifting the jet stream southward to around 30°N.

After 11 February, the eastern North Pacific ridge, North American TPV, and Arctic positive GHT anomaly began weakening. However, a wave train developed from the western North Pacific low center to North America, maintaining the ridge over the eastern North Pacific and the trough over the Great Plains and the Southern United States for an extended time period (up to 18 February). Due to the relatively southern location of the wave train (particularly the two low centers), the jet stream shifted south of 30°N in the United States, which is unusual, and led to the disastrous and persistent cold weather in Texas and the adjacent states.

So far, we have analyzed the spatial structures and temporal evolutions of the tropospheric circulation anomalies, which have triggered and steered cold polar air outbreaks. However, a number of questions remain open regarding the changes in the tropospheric circulations, including (1) why the wave train was deformed and the North Atlantic low anom-

aly center shifted southward in the first East Asia cold event; (2) what additional force drove the intensification of the East Asian trough in the second East Asian event; and (3) why the TPV intensified and moved southward in the North American event. We address these questions below through examining stratosphere–troposphere interactions.

4.3. *Sudden stratospheric warming and stratospheric polar vortex*

The stratospheric atmosphere also experienced tremendously large anomalies in winter 2020/21. In climatology, the SPV emerges and then intensifies in the fall and weakens and dissipates in the spring. During this course, it reaches its strongest state in January with the lowest GHT. However, the 50 hPa GHT dramatically increased from late December 2020 to mid-February 2021 (Fig. 5), coincident with the period of the three extreme cold events shown above. It departed from its climatology by more than one standard deviation and even exceeded two standard deviations in mid-January, indicating an occurrence of a major sudden stratospheric warming (SSW) event with a weakened SPV.

The SSW event and its extended persistence in winter 2020/21 could be ascribed to the increase in the tropospheric poleward transient eddy heat transport, which is the source of the wave activity (e.g., Edmon et al., 1980). As shown in Fig. 4, a GHT ridge and a poleward propagating Rossby wave train occurred on 25–26 December 2020, resulting in a heat flux intrusion from the North Atlantic into the Arctic and, in turn, substantially decreasing sea ice cover in the Barents–Kara seas. The anomalous poleward heat intrusion and the decreased sea ice cover over the warm ocean would also increase atmospheric transient eddy heat flux, which is the mechanism inducing an upward propagation of planetary Rossby waves to disrupt the SPV. In particular, the long memory of the retreated sea ice and the underlying warm ocean can favorably maintain surface and lower tropospheric warming and, therefore, increase transient eddy heat flux over a longer time period, supporting a persistence of the SSW event. This role of decreased sea ice in disrupting the SPV through planetary Rossby waves was revealed through data analysis and modeling experiments in Kim et al. (2014) and Zhang et al. (2018a). In addition, during the second East Asian event and the North American event, the intermittently occurring blocking highs, or ridges, from the North Atlantic, the eastern North Pacific, and eastern Canada–Baffin Bay would also continually reinforce the wave activity, sustaining the SSW event for a long time (about one and half months).

As a consequence of the SSW event, the weakened SPV demonstrated a deformation in its spatial structure, which can intensify the tropospheric circulation anomalies to cause the extreme cold events. We now discuss these processes in each of the three events. During the first East Asian event, the SPV center was displaced to be over the Eurasian continent with a deep trough located from Scandinavia to Western Europe. It reached its strongest state on 28 December 2020 (Fig. 6a). In correspondence to the maximum negative GHT anomaly at 50 hPa, a positive potential vorticity (PV) anomaly, which is defined by the local maximum of PV, would develop. According to PV dynamics (Hoskins, et. al., 1985), the positive PV anomaly spun up cyclonic circulation underneath itself, generated a jet stream under the tropopause, and supported enhancement of tropospheric baroclinicity, which finally intensified the tropospheric low pressure system. This downward impact mechanism explains the shift of the anomalous tropospheric low center from the northwestern North Atlantic to the area over the United Kingdom, as shown in Figs. 4a2–a3. This shift facilitated the wave train propagation from the North Atlantic to East Asia and, in turn, amplified meridional circulation to cause a cold air outbreak in East Asia.

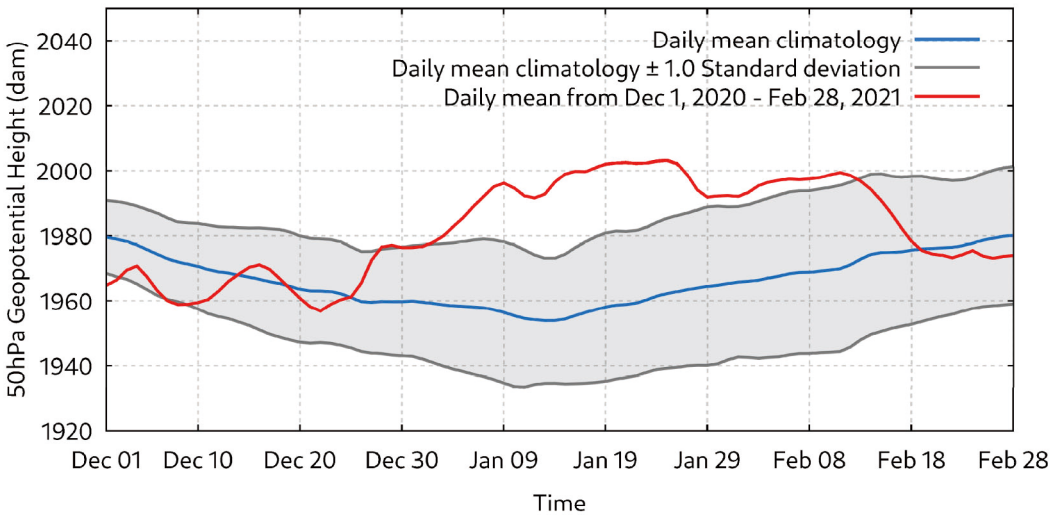

Fig. 5. Winter (1 December–28 February) climatology (blue line) and one standard deviation (grey lines and shading) of variability of the polar cap (60°–90°N) area-averaged daily mean geopotential height (Units: dam) at 50 hPa from 1979/80–2008/09. The red line shows the daily mean polar cap area-averaged geopotential height at 50 hPa from 1 December 2020–28 February 2021.

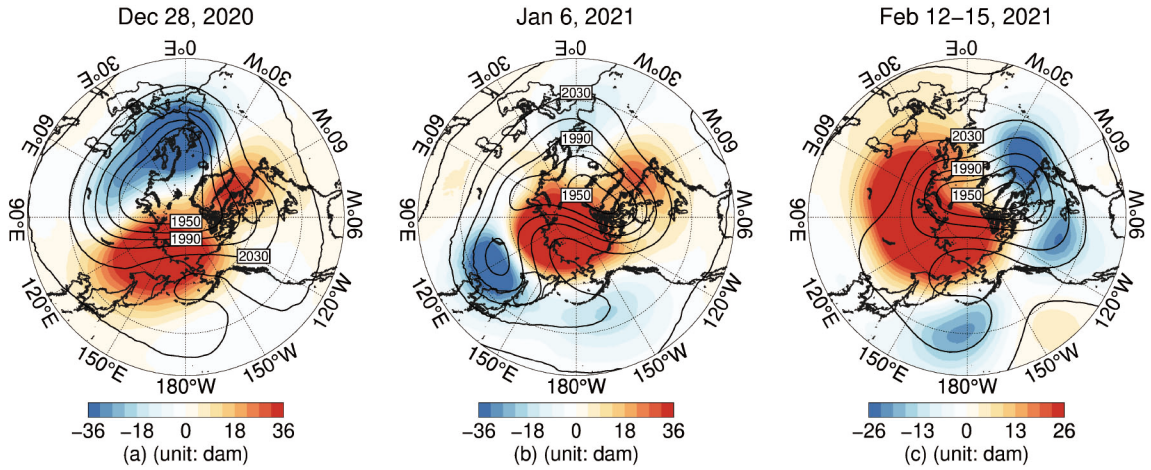

Fig. 6. Daily mean geopotential height (GHT; contours) and GHT anomalies (shading) at 50 hPa on (a) 28 December 2020 and (b) 6 Janauary 2021. (c) Average of daily mean GHT and daily mean GHT anomalies during 12–15 Feburary 2021. The daily GHT anomalies were calcuated relative to the daily GHT climatology constructed from 1979/80–2008/09. Units: dam.

The SSW persisted into the second East Asian event. The weakened SPV evolved to be split to two daughter centers (or vortices) situated over Greenland and Northeast Asia, respectively (Fig. 6b). The latter center was stronger than the former one and showed a maximum negative GHT anomaly at 50 hPa. Similar to the PV dynamic processes discussed above, the Northeast Asian center and associated positive PV anomaly would deepen the anomalous tropospheric low center, or the corresponding East Asian trough, and strengthen the jet stream at the bottom of the trough (Figs. 4b4–b6), amplifying the meridional flow and, in turn, driving the cold polar airmass to spread southward.

The role of the SSW in the development of the North American cold event exhibited differences from those of the two East Asian events. In the East Asian events, the dispaced or split SPV center mainly modulated or intensified tropospheric circulation anomalies at one particular step/phase. However, the weakened SPV progressively played a role in the tropospheric circualtion changes from the begining throughout most of the time during the occurrence and development of the North America event. The SPV was still split into two centers over the western North Pacific and Baffin Bay–Greeland, respectively (Fig. 6c). In early Feburary 2021, the Baffin Bay–Greeland SPV center intensified and meridionally stretched the anomalous tropospheric low center of the PNA pattern following the same downward impact theory mentioned above (Figs. 4c1 and c2). This also strengthened the tropospheric blocking high over the eastern North Pacific and the trough over North America, as shown in Figs. 4c1–c2. Subsequently, both the North America and western North Pacific SPV centers extended considerablly southward, leading to negative GHT anomaly centers at 50 hPa located as far south as 30°N. Under the influence of the two SPV centers, the two underneath tropospehric low GHT centers intensified, and a wave train developed in the far south propagating from the western North Pacific to south of the Great Plains. The jet stream was also located anomalously farther south than its climatology (Figs. 4c3–c6). Therefore, this circuation pattern continously steered snow/ice storms along with cold temperatures toward the southern United States.

5. Summary and future implications

We analyzed the three striking extreme cold weather events occurring over East Asia and North America during the mid-winter of 2020/21. Statistical analysis indicates extremeness of these events at the 2nd, 3rd, and 1st percentiles of all winter daily mean temperature anomaly events since 1979/80. The most prominent feature of each of these events is the southward extent of cold polar air reaching climatologically warmer areas, particularly in North America, breaking many historical cold temperature records. A PDF analysis further suggests that, although the warming trend during the most recent decade increased the frequency of occurrence of warm temperature events in both East Asia and North America and decreased the frequency of cold temperature events in North America, the probability of occurrence of severe winter cold events in East Asia was unchanged.

Based on well-established fundamental atmospheric dynamics and recent research findings (e.g., Edmon et al., 1980; Hoskins et al., 1985; van den Dool et al., 2000; Holton, 2004; Kim et al., 2014; Zhang et al., 2018a), we quantified anomalous ocean thermal forcing and atmospheric circulation anomalies in both the troposphere and stratosphere and inferred underlying quantitative physical processes from the circulation anomalies. The results suggest that the occurrence and persistence of these three events can be attributed to the integrated effects of the concurrence of anomalous ocean thermal conditions in the North Atlantic Ocean and the Pacific Ocean and the large sea ice retreat over the warm Barents–Kara seas. Obviously, the North Atlantic warm blob played an initiating role in increasing poleward transient eddy heat flux through a corres-

ponding ridge and a follow-up Rossby wave train into the North Atlantic Arctic. This initiation triggered two pathways to cause the three extreme events to successively occur. First, the increased transient eddy heat flux, or the wave activity, excited upward propagation of the planetary waves to disrupt the SPV and caused a major SSW event to occur, building up a stratospheric pathway. Second, the Rossby wave trains, induced by the North Atlantic warm blob and the tropical Pacific La Niña event, propagated to East Asia and to North America, respectively, and interacted with the Arctic tropospheric circulation anomalies, or the TPV, setting up a tropospheric pathway. The long memory of the retreated Barents–Kara seas sea ice, with the underlying warm ocean and the amplified blocking highs extending from the midlatitudes to the Arctic along the tropospheric pathway, intermittently fueled the increased transient eddy heat flux during the three events, sustaining the SSW over a long time period. Meanwhile, the displaced or split SPV centers feed back to the troposphere, modulating the wave trains or intensifying the tropospheric circulation anomalies through downward impact mechanism, leading the cold events to an extreme state.

Although all three events were linked under the influence of one major SSW event, the SPV downward impact mechanism took effect differently in each case. In the first East Asia event, the SPV showed a displacement of its spatial structure. The displaced deep SPV trough from Scandinavia to Western Europe re-oriented the wave train to propagate in the midlatitudes from the North Atlantic to East Asia, providing a dynamic setting to steer cold polar air southward in East Asia. In the second East Asia event, the split SPV center over East Asia predominantly intensified the East Asian trough in the troposphere, shaping a strong, meridionally aligned circulation with the anomalous Arctic high. The split SPV center over North America played a crucial role, from initiation throughout most of the lifetime of the cold event, in driving intensification and a southward shift of the tropospheric low center, which caused extensive deepening of the tropospheric trough into the southern United States.

We also noticed that the occurrence of the extreme events was obviously driven by multiple factors associated with surface forcing and atmospheric circulation elements, as stated in recent reviews (e.g., Cohen et al., 2020; Vihma et al., 2020; Zhang et al., 2020; Overland et al., 2021). Taking one more step forward, we would like to emphasize that systematic, hemispheric-scale changes in the atmospheric circulation are essential in causing the occurrence of massive, long-lasting extreme events at large spatial scales or across the Northern Hemisphere. These systematic changes can be an integration of (1) a concurrence of multiple surface thermal forcing mechanisms in multiple ocean basins; and (2) interactions between high-lower latitudes and troposphere–stratosphere atmospheric dynamic processes. Most current studies focus mainly on detecting a sole forcing-effect relationship between sea ice and atmospheric circulation anomalies without inclusion of other concurrent ocean forcing mechanisms and essential interactive atmospheric processes. This could be the source of the large uncertainties, which has driven the strong debates on the topic. For instance, Zhang et al. (2008) identified a systematic, coherent transformation of the hemispheric-scale atmospheric circulation characterized by a strengthened/northward expanded Siberian high and a deepened Aleutian low, which enhances poleward heat transport from the North Atlantic to the Arctic and drives a simultaneous occurrence of rapid Arctic warming/sea ice decrease and Eurasian cooling. During the process of this transformation, there is no doubt about positive feedbacks from the retreated sea ice and warmed ocean to the overlying atmospheric circulation to support its polarization and persistence. Although the transformation of the circulation mentioned above was revealed using monthly data, the daily temporal evolution of the atmospheric circulation and the consequent spatial patterns of the GHT anomalies in the two East Asia events showed the same systematic changes on the hemispheric scale, instead of independent, local circulation anomalies.

It is worthwhile to disentangle the large-scale, monthly/seasonal circulation changes by examining a single circulation element or weather system over a particular region, which is important to better understand and predict daily evolution and associated spatial distribution of circulation anomalies. However, we should note from the analysis here that a single circulation element, such as a blocking high, is also highly dynamic and may not stationarily occur in one particular region. This would be the reason that statistically significant trends of the Ural Mountains/Greenland blocking highs have not been detected when examining their role in the increased extreme cold events (e.g., Overland et al., 2021).

Here we provide an insightful view of the physical processes that would predominantly play driving roles in the occurrence of the three events as summarized in Fig. 7. All changes and anomalies of the atmospheric circulation have been examined in this analysis. The underlying physical processes and mechanisms are complex. Although we have qualitatively inferred them from the analyzed atmospheric anomalies (including those not shown here, such as 3D air temperatures) based on atmospheric dynamics and recent research findings, detailed quantitative analysis and modeling sensitivity experiments would be an important follow-up to accurately verify/refine these processes and get in-depth understanding of their relative roles in the different phases governing evolution of the atmospheric circulation. The processes suggested in Fig. 7 would therefore be a starting point to further foster research and discussions on the topic in the research community.

The analysis of these three events in this study and other ongoing studies would have significant implications for better understanding the sources of predictability of winter extreme cold events. There have been ongoing efforts to improve prediction of the Arctic–midlatitude linkage and resultant midlatitude extreme events (e.g., Jung et al., 2016; Collow et al., 2018; Zhang et al., 2018b; Dai and Mu, 2020). Correctly identifying original and subsequent surface forcing mechanisms and cap-

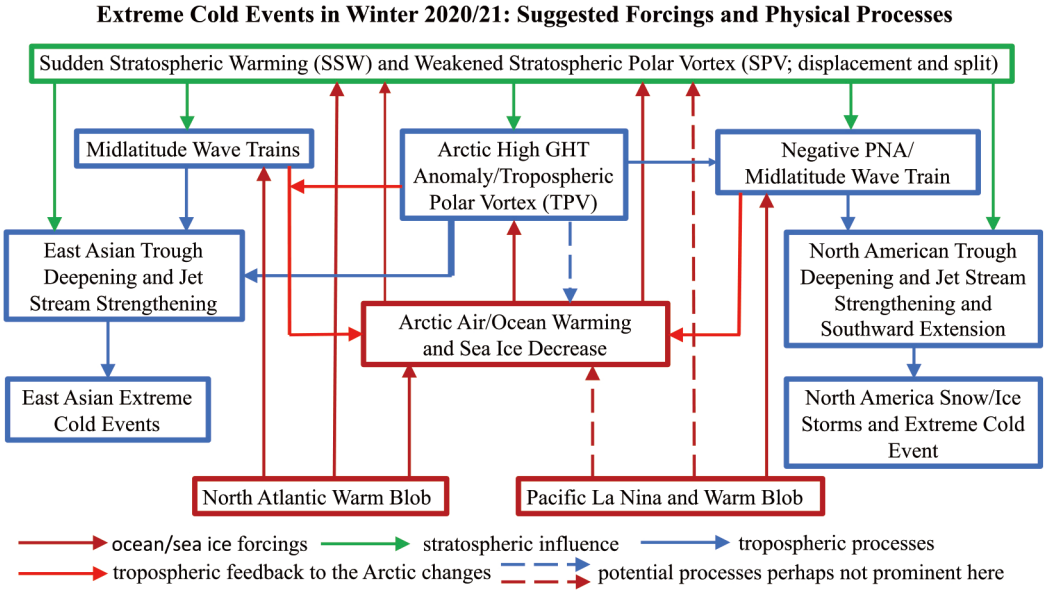

Fig. 7. Schematic diagram illustrating the suggested ocean–sea ice thermal forcing mechanisms and the prominent influencing and interactive physical processes for the occurrence of the three extreme cold events in winter 2020/21. The ocean–sea ice forcing mechanisms and atmospheric circulation elements and anomalies shown in the boxes are well revealed in the analysis in Figs. 3–6. The suggested physical processes and mechanisms indicated by the solid arrows are inferred from the atmospheric anomalies based on well-established fundamental dynamics theory and recent research findings, which would guide detailed quantitative analysis and model sensitivity experiments for further accurate evaluation and refinement.

turing atmospheric interactive processes are important for strategizing and designing model initialization and observational data assimilation, which are critical for improving model predication skill.

In addition, the global warming is continuing year-by-year, while extreme events occur intermittently. Interactions between the long-term warming and natural variability would be important to influence occurrence, intensity, and duration of extreme events, as shown in this analysis. For instance, Arctic sea ice will be continually thinning under future global warming scenarios. It therefore becomes more vulnerable to melt, drift, and deformation in response to anomalous heat and momentum input from atmospheric circulation changes induced by lower latitude ocean forcing. This would spatially or temporally alter generation of wave activity and, in turn, the strength of the SPV, influencing the interactions between the stratosphere and troposphere and the frequency of occurrence of extreme events. It is therefore important to assess future potential forcing mechanisms in all ocean basins, along with the emergent forcing from the amplified warming/rapid decrease in sea ice in the Arctic Ocean. This would benefit planning and policy-making for mitigating impacts of this type of extreme event on human–ecosystem–environmental health and socioeconomics, moving the world towards enhanced resilience in the "One Health, One Future".

Acknowledgements. The Copernicus Climate Change Service (C3S), NOAA, and NSIDC provided the ERA5, ERSST v5, and sea ice concentration data used in this study. This study was supported by the U.S. Department of Energy (Grant No. DE-SC0020640), the National Natural Science Foundation of China (Grant Nos. 41675041 and 41790475), the Arctic Research Program of the NOAA Global Ocean Monitoring and Observing Office, the Deutsche Forschungsgemeinschaft (project 268020496 TRR 172 within the Transregional Collaborative Research Center "ArctiC Amplification: Climate Relevant Atmospheric and SurfaCe Processes, and Feedback Mechanisms (AC)3"), the Academy of Finland (contract 317999), and the Cooperative Institute for Climate, Ocean, & Ecosystem Studies (CIOCES) under NOAA Cooperative Agreement NA20OAR4320271. This is PMEL contribution 5269 and CIOCES contribution 2021-1151.

REFERENCES

Barnes, E. A., and L. M. Polvani, 2015: CMIP5 projections of Arctic amplification, of the North American/North Atlantic circulation, and of their relationship. *J. Climate*, **28**, 5254–5271, https://doi.org/10.1175/JCLI-D-14-00589.1.

Barnes, E. A., and J. A. Screen, 2015: The impact of Arctic warming on the midlatitude jet-stream: Can it? Has it? Will it? *WIREs Climate Change*, **6**, 277–286, https://doi.org/10.1002/wcc.337.

Basu, S., X. D. Zhang, I. Polyakov, and U. S. Bhatt, 2013: North American winter-spring storms: Modeling investigation on tropical Pacific sea surface temperature impacts. *Geophys. Res. Lett.*, **40**, 5228–5233, https://doi.org/10.1002/grl.50990.

Blackport, R., and J. A. Screen, 2020: Insignificant effect of Arctic amplification on the amplitude of midlatitude atmospheric waves. *Sci-*

ence Advances, **6**, eaay2880, https://doi.org/10.1126/sciadv.aay2880.
Cavalieri, D. J., C. L. Parkinson, P. Gloersen, and H. J. Zwally, 1996: Sea Ice Concentrations from Nimbus-7 SMMR and DMSP SSM/I-SSMIS Passive Microwave Data, Version 1. Boulder, Colorado USA. NASA National Snow and Ice Data Center Distributed Active Archive Center. Available from https://doi.org/10.5067/8GQ8LZQVL0VL.
Cohen, J., and Coauthors, 2020: Divergent consensuses on Arctic Amplification influence on midlatitude severe winter weather. *Nature Climate Change*, **10**, 20–29, https://doi.org/10.1038/s41558-019-0662-y.
Collow, T. W., W. Q. Wang, and A. Kumar, 2018: Simulations of Eurasian winter temperature trends in coupled and uncoupled CFSv2. *Adv. Atmos. Sci.*, **35**, 14–26, https://doi.org/10.1007/s00376-017-6294-0.
Dai, G. K., and M. Mu, 2020: Arctic influence on the eastern Asian Cold Surge Forecast: A case study of January 2016. *J. Geophys. Res.*, **125**, e2020JD033298, https://doi.org/10.1029/2020JD033298.
Edmon, H. J. Jr., B. J. Hoskins, and M. E. McIntyre, 1980: Eliassen-Palm cross sections for the troposphere. *J. Atmos. Sci.*, **37**, 2600–2616, https://doi.org/10.1175/1520-0469(1980)037<2600:EPCSFT>2.0.CO;2.
Francis, J. A., and S. J. Vavrus, 2015: Evidence for a wavier jet stream in response to rapid Arctic warming. *Environmental Research Letters*, **10**, 014005, https://doi.org/10.1088/1748-9326/10/1/014005.
Hanna, E., T. E. Cropper, R. J. Hall, and J. Cappelen, 2016: Greenland blocking index 1851–2015: A regional climate change signal. *International Journal of Climatology*, **36**, 4847–4861, https://doi.org/10.1002/joc.4673.
Hersbach, H., and Coauthors, 2020: The ERA5 global reanalysis. *Quart. J. Roy. Meteor. Soc.*, **146**, 1999–2049, https://doi.org/10.1002/qj.3803.
Holton, J. R., 2004: An Introduction to Dynamic Meteorology. 4th ed. Elservier Academic Press.
Hoskins, B. J., M. E. McIntyre, and A. W. Robertson, 1985: On the use and significance of isentropic potential vorticity maps. *Quart. J. Roy. Meteor. Soc.*, **111**, 877–946, https://doi.org/10.1002/qj.49711147002.
Huang, B., and Coauthors, 2017a: Extended Reconstructed Sea Surface Temperature, Version 5 (ERSSTv5): Upgrades, validations, and intercomparisons. *J. Climate*, **30**, 8179–8205, https://doi.org/10.1175/JCLI-D-16-0836.1.
Huang, J. B., and Coauthors, 2017b: Recently amplified arctic warming has contributed to a continual global warming trend. *Nature Climate Change*, **7**, 875–879, https://doi.org/10.1038/s41558-017-0009-5.
Jung, T., and Coauthors, 2016: Advancing polar prediction capabilities on daily to seasonal time scales. *Bull. Amer. Meteor. Soc.*, **97**, 1631–1647, https://doi.org/10.1175/BAMS-D-14-00246.1.
Kim, B.-M., S.-W. Son, S.-K. Min, J.-H. Jeong, S.-J. Kim, X. D. Zhang, T. Shim, and J.-H. Yoon, 2014: Weakening of the stratospheric polar vortex by Arctic sea-ice loss. *Nature Communications*, **5**, 4646, https://doi.org/10.1038/ncomms5646.
Kretschmer, M., J. Cohen, V. Matthias, J. Runge, and D. Coumou, 2018: The different stratospheric influence on cold-extremes in Eurasia and North America. *npj Climate and Atmospheric Science*, **1**, 44, https://doi.org/10.1038/s41612-018-0054-4.
Luo, D., Y. Xiao, Y. Diao, A. Dai, C. L. E. Franzke, and I. Simmonds, 2016: Impact of Ural blocking on winter warm Arctic-cold Eurasian anomalies. Part II: The link to the North Atlantic Oscillation. *J. Climate*, **29**, 3949–3971, https://doi.org/10.1175/JCLI-D-15-0612.1.
Maslanik, J., and J. Stroeve, 1999: Near-Real-Time DMSP SSMIS Daily Polar Gridded Sea Ice Concentrations, Version 1. Boulder, Colorado USA. NASA National Snow and Ice Data Center Distributed Active Archive Center. Available from https://doi.org/10.5067/U8C09DWVX9LM.
McCusker, K. E., J. C. Fyfe, and M. Sigmond, 2016: Twenty-five winters of unexpected Eurasian cooling unlikely due to Arctic sea-ice loss. *Nature Geoscience*, **9**, 838–842, https://doi.org/10.1038/ngeo2820.
Overland, J., J. A. Francis, R. Hall, E. Hanna, S.-J. Kim, and T. Vihma, 2015: The melting Arctic and midlatitude weather patterns: Are they connected? J *Climate*, **28**, 7917–7932, https://doi.org/10.1175/JCLI-D-14-00822.1.
Overland, J. E., and Coauthors, 2021: How does the Arctic influence midlatitude winter extreme weather events? *Environmental Research Letters*, **16**, 043002, https://doi.org/10.1088/1748-9326/abdb5d.
Screen, J. A., and Coauthors, 2018: Consistency and discrepancy in the atmospheric response to Arctic sea-ice loss across climate models. *Nature Geoscience*, **11**, 155–163, https://doi.org/10.1038/s41561-018-0059-y.
Thompson, D. W. J., and J. M. Wallace, 1998: The Arctic Oscillation signature in the wintertime geopotential height and temperature fields. *Geophys. Res. Lett.*, **25**, 1297–1300, https://doi.org/10.1029/98GL00950.
Tyrlis, E., E. Manzini, J. Bader, J. Ukita, H. Nakamura, and D. Matei, 2019: Ural blocking driving extreme Arctic Sea Ice loss, cold Eurasia, and stratospheric vortex weakening in autumn and early winter 2016-2017. *J. Geophys. Res.*, **124**, 11 313–11 329, https://doi.org/10.1029/2019JD031085.
van den Dool, H. M., S. Saha, and Å. Johansson, 2000: Empirical orthogonal teleconnections. *J. Climate*, **13**, 1421–1435, https://doi.org/10.1175/1520-0442(2000)013<1421:EOT>2.0.CO;2.
Vavrus, S. J., F. Y. Wang, J. E. Martin, J. A. Francis, Y. Peings, and J. Cattiaux, 2017: Changes in North American atmospheric circulation and extreme weather: Influence of Arctic Amplification and Northern Hemisphere snow cover. *J. Climate*, **30**, 4317–4333, https://doi.org/10.1175/JCLI-D-16-0762.1.
Vihma, T., and Coauthors, 2020: Effects of the tropospheric large-scale circulation on European winter temperatures during the period of amplified Arctic warming. *International Journal of Climatology*, **40**, 509–529, https://doi.org/10.1002/joc.6225.
Woollings, T., and Coauthors, 2018: Daily to decadal modulation of jet variability. *J. Climate*, **31**, 1297–1314, https://doi.org/10.1175/JCLI-D-17-0286.1.
Wu, Q. G., and X. D. Zhang, 2010: Observed forcing-feedback processes between northern hemisphere atmospheric circulation and Arctic sea ice coverage. *J. Geophys. Res.*, **115**, D14119, https://doi.org/10.1029/2009JD013574.
Yamazaki, K., T. Nakamura, J. Ukita, and K. Hoshi, 2020: A tropospheric pathway of the stratospheric quasi-biennial oscillation (QBO)

impact on the boreal winter polar vortex. *Atmospheric Chemistry and Physics*, **20**, 5111–5127, https://doi.org/10.5194/acp-20-5111-2020.

Zhang, P. F., Y. T. Wu, I. R. Simpson, K. L. Smith, X. D. Zhang, B. De, and P. Callaghan, 2018a: A stratospheric pathway linking a colder Siberia to Barents-Kara Sea sea ice loss. *Science Advances*, **4**, eaat6025, https://doi.org/10.1126/sciadv.aat6025.

Zhang, X., A. Sorteberg, J. Zhang, R. Gerdes, and J. C. Comiso, 2008: Recent radical shifts in atmospheric circulations and rapid changes in Arctic climate system. *Geophys. Res. Lett.*, **35**, L22701, https://doi.org/10.1029/2008GL035607.

Zhang, X., C. H. Lu, and Z. Y. Guan, 2012: Weakened cyclones, intensified anticyclones and recent extreme cold winter weather events in Eurasia. *Environmental Research Letters*, **7**, 044044, https://doi.org/10.1088/1748-9326/7/4/044044.

Zhang, X., T. Jung, M. Y. Wang, Y. Luo, T. Semmler, and A. Orr, 2018b: Preface to the special issue: Towards improving understanding and prediction of arctic change and its linkage with Eurasian mid-latitude weather and climate. *Adv. Atmos. Sci.*, **35**, 1–4, https://doi.org/10.1007/s00376-017-7004-7.

Zhang, X. D., Y. F. Fu, Z. Y. Guan, H. Tang, G. M. Wang, Z. M. Wang, P. L. Wu, and X. Q. Yang, 2020: Influence of Arctic warming amplification on Eurasian winter extreme weather and climate: Consensus, open questions, and debates. *Journal of the Meteorological Sciences*, **40**, 596–604, https://doi.org/10.3969/2020jms.0079. (in Chinese with English abstract)